

# The Complementary Nature of X-Ray Photoelectron Spectroscopy and Angle-Resolved X-Ray Diffraction

## Part I: Background and Theory

S.J. Kerber, T.L. Barr, G.P. Mann, W.A. Brantley, E. Papazoglou, and J.C. Mitchell

(Submitted 6 November 1997; in revised form 12 February 1998)

**X-ray photoelectron spectroscopy (XPS) and x-ray diffraction (XRD) are often used to analyze the surface of complex oxide materials. When XRD is used in an atypical angle resolved x-ray diffraction (ARXRD) mode, crystalline composition as a function of depth can be obtained. Similarly, when XPS is used in conjunction with argon depth profiling, composition as a function of depth can also be obtained. A review of the two techniques is included, comparing and contrasting their ability to obtain chemical information as a function of depth for heterogeneous oxide layers. The novel, simultaneous implementation of these two techniques is a unique combination of procedures that can provide substantial amounts of information about the composition of complex oxides.**

**Keywords** angle-resolved, depth profile, oxide, review, x-ray diffraction, x-ray photoelectron spectroscopy

## 1. Introduction

### 1.1 General

Oxide layers exist on almost all surfaces exposed to the atmosphere, even at room temperature. When temperatures are increased, the oxide layer can be thick—up to several micrometers. Some examples include corrosion products, Kovar oxidation before glass joining, pretreatments for subsequent painting of surfaces, and passivated stainless steels. These layers are usually not homogeneous, in either lateral or depth dimensions. The analysis of these complex oxides is important because it not only gives information as to the fundamental behavior of materials, but also yields more cost-efficient engineering processes.

Both x-ray diffraction (XRD) and x-ray photoelectron spectroscopy (XPS, also known as ESCA, electron spectroscopy for chemical analysis) are commonly used to analyze these types of oxide layers (Ref 1-6). In theory, XRD identifies crystalline materials within about 10  $\mu\text{m}$  of the surface. The expanded technique of angle-resolved x-ray diffraction (ARXRD) utilizes a fixed x-ray source with a scanning detector; in the scientific literature this technique is generally termed grazing-angle x-ray diffraction (Ref 7-12). If the source is set at a very shallow

glancing angle, the x-rays detected are from a near-surface region of a few tens of nanometers. As the incident angle increases, the signal is obtained from an increasing depth of the material. Toney and Huang (Ref 10) reported using grazing angle for depth profiling by varying the x-ray source incidence angle from  $0.329^\circ$  to  $0.519^\circ$ . Similarly, Neerincx and Vink (Ref 9) used incident angles of  $0.3^\circ$ ,  $0.45^\circ$ ,  $0.7^\circ$ , and  $5^\circ$  to depth profile indium tin oxide (ITO) films. In the study in Part II of this report (Ref 13), the x-ray source was varied from grazing values of  $<1^\circ$  to incident angles of  $20^\circ$ , which can no longer be defined as grazing. The ARXRD terminology was chosen because of its correspondence to the use of angle-resolved XPS for depth profiling of surface layers from 2 to 8 nm (Ref 14). When XPS, which typically analyzes a depth of 5 nm, is combined with argon ion depth profiling, chemical information as a function of depth is also obtained, typically to maximum depths of a few hundred nanometers. In practice, the analysis of complex oxides with either of these techniques can be less than straightforward. However, it has been determined that a combination of the two techniques can be used to minimize shortcomings of the individual methods if the backgrounds of the procedures are fully understood and the merging of the data is done with caution (Ref 13).

### 1.2 XPS Theory

In XPS, a sample is irradiated with monoenergetic soft x-rays and the emitted electrons are energy analyzed. The x-rays are typically either aluminum  $K\alpha$  or magnesium  $K\alpha$  with energies of 1486.7 eV and 1253.6 eV, respectively. The emitted photoelectrons, generated within about 5 nm of the surface, have a measured kinetic energy,  $KE$ , given by:

$$KE = h\nu - BE - \phi_s \quad (\text{Eq 1})$$

where  $h\nu$  is the energy of the photon,  $BE$  is the binding energy of the atomic orbital from which the emitted electron originates, and  $\phi_s$  is the spectrometer work function. Because each

**S.J. Kerber**, Material Interface, Inc., N73W22301 Willowview Drive, Sussex, WI 53089-2244, e-mail: matlinter@aol.com; **T.L. Barr** and **G.P. Mann**, Department of Materials, Laboratory for Surface Studies, University of Wisconsin-Milwaukee, Milwaukee, WI, 53201; e-mail: terybarr@csd.uwm.edu; **W.A. Brantley** and **E. Papazoglou**, Section of Restorative Dentistry, Prosthodontics and Endodontics, College of Dentistry, The Ohio State University, Columbus, OH 43210-1241, e-mail: brantley.1@osu.edu, papazoglou.1@osu.edu; **J.C. Mitchell**, Microscopic and Chemical Analysis Research Center, Department of Geological Sciences, The Ohio State University, Columbus, OH 43210-1308, e-mail: mitchell.3@osu.edu.

element has a unique set of binding energies, XPS can be used to identify and determine the concentration of the elements at the surface. Subtle variations in the binding energies can be used to identify the chemical state of the materials being analyzed. When monochromatic aluminum x-rays are used as the source, increased energy resolution is obtained which aids in the identification of surface species. In addition to the photoelectrons emitted, Auger electrons are also emitted because of relaxation of the excited ions remaining after photoemission.

In practice, a survey scan is initially obtained in the binding energy range from ~1200 to 0 eV. This is performed to determine which elements above the atomic number 2 are present. Each element for which binding energy information is required has a narrow window (typically about 20 eV) about the central peak analyzed in a high energy resolution mode to determine the binding energy of the surface species and make determinations of the compounds present. The data are compared to either published literature values of known standards (Ref 15-17) or to theoretical arguments based upon chemical bonding (Ref 18). It is not uncommon for literature values of desired species to be nonexistent; therefore, identification can be less than straightforward.

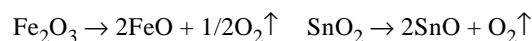
Quantitative analysis of XPS data can be accomplished via elemental sensitivity factors (Ref 16, 19). These values are normalization factors based upon calculated yields for pure elements. In compounds and complex oxides, the sensitivity factors are not necessarily valid, and the concentration information obtained should be taken to be semiquantitative at best and most properly used for comparisons only.

For "clean" metallic samples exposed to the atmosphere, levels of 10 to 20% carbon and 30 to 50% oxygen are typical. Primarily, the carbon is due to adsorbed hydrocarbons and carbon oxides (commonly called adventitious carbon), and the oxygen is due to instantaneous oxide formation and adsorbed water vapor. A clean metallic surface is very reactive and will adsorb more water vapor than a contaminated surface. Metals generally adsorb more atmospheric contaminants than ceramic materials.

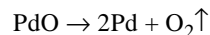
When concentration as a function of depth is desired, the sample can be sputtered with argon ions to remove material from the surface. As material is removed, the analysis is repeated. This method can be complicated by preferential sputtering, a process in which the ion etching of a multicomponent system may result in the faster ejection of one of the components compared to that of the others. For example, the relative sputter rate of gold can be four times that of silicon (Ref 16). Preferential sputtering may occur in the case of an alloy or even for a chemical compound. In the latter case, it generally involves the preferential removal of some or all of the anionic species and therefore is often collectively described as sputter reduction. Preferential sputtering often arises due to significant differences in atomic mass or as a result of relatively low bond energy stabilization (Ref 20, 21). In any case, it is a fairly common problem in examining mixed systems, particularly when oxides are involved.

Ion etching of oxides with Ar<sup>+</sup> generally produces some microstructural alteration (producing defect sites) and often preferentially removes oxygen compared to the rate of ejection of the corresponding cations (Ref 21). The sputter reduction of

oxides is most prominent in cases where stable suboxides are common:



and also when the thermal stability of an oxide is low:



As a result of preferential sputtering, it is often difficult to employ the method of profiling to obtain an accurate identification of the true subsurface composition. It should be kept in mind, however, that only the relatively unstable oxides sputter reduce to their elemental metal. No sputter reduction process goes to 100% completion.

Depth profile rates are typically calibrated to carefully prepared thin film samples, often SiO<sub>2</sub> or Ta<sub>2</sub>O<sub>5</sub> (Ref 16). In the case of heterogeneous oxide layers, perfect thin film standards generally do not exist. Relative depth measurements (as a function of sputtering time) are the best that can be accomplished, with the depth profile rate from the thin film standard used as a general guideline. Similarly, engineered samples are never perfectly smooth. During ion bombardment of rough samples, one must be aware that some shadowing will occur, and little or no material will be removed from the shadowed surfaces. Additionally, extensive depth profiling can produce roughness of its own (Ref 22). Once again, comparisons between similar samples is an important consideration.

Despite the concerns listed above, XPS should be considered as one of the most valuable options for the analysis of complex oxides. An understanding of the considerations helps to enhance the interpretation of the data obtained.

### 1.3 ARXRD Theory

Because crystals are symmetrical arrays of atoms containing parallel planes of spacing similar to the linewidth  $\lambda$  of common characteristic x-rays, they can act as a diffraction grating for these x-rays. Depending upon the crystal structure, constructive or destructive interference with an x-ray beam can occur. During constructive interference conditions, Bragg's law will apply:

$$n\lambda = 2d\sin\theta \quad (\text{Eq 2})$$

where  $n$  is the order of the diffraction (1, 2, 3...),  $\lambda$  is the x-ray wavelength in Å,  $d$  is the crystal interplanar spacing, and  $\theta$  is the angle of incidence or reflection of the x-ray beam. The ideal crystal size for Bragg reflection is about 10<sup>-3</sup> cm. If crystals are too small, that is, less than ~10<sup>-6</sup> cm, diffuse scattering occurs rather than Bragg reflections (Ref 23). Between these ranges, smaller crystallites cause broadening of peaks that are obtained. Nonuniform strain also results in broadened peaks. If there is uniform strain in a material, the  $d$ -spacing changes, and peak locations are shifted accordingly.

During angle-resolved x-ray diffraction (ARXRD), the x-ray source is held at fixed angles that vary from grazing geometries toward normal incidence. In the traditional  $\theta/2\theta$  XRD geome-

try, the planes that contribute to diffraction are always parallel to the surface. In the glancing angle, fixed source geometry, there is a specific focusing radius for each  $2\theta$  value. To maintain focusing over the entire  $2\theta$  range, one translates the receiving slit and detector assembly parallel to the diffracted beam as the  $2\theta$  angle is varied. The angular divergence slits are placed in front of the detector so that only the parallel rays diffracted from the sample will be accepted into the detector.

In order to determine the ARXRD depth of analysis,  $\Phi(x)$  (the fraction of the total diffracted intensity contributed by a composite surface layer at a depth  $x$ ) is plotted as a function of  $x$  for a given incident angle  $\alpha$  according to the following expression:

$$\Phi(x) = 1 - e^{-\mu x [1/\sin \alpha + 1/\sin (2\theta - \alpha)]} \quad (\text{Eq 3})$$

where  $\mu$  is the mass absorption coefficient of the material and  $2\theta$  is the angle of the diffracted peak of interest and  $e$  is the exponential constant. For a given material, x-rays related to different  $2\theta$  values are diffracted at different depths, as illustrated in Fig. 1. The detection depth is then classified as a  $1/e$  depth, when 63% of the diffracted intensity is obtained compared to the bulk (Ref 24).

## 2. Experimental

Experiments were performed to compare empirically determined analysis depths to depths calculated using Eq 3. A sample that was nominally 50 nm gold over 200 nm platinum deposited on an oxidized silicon wafer was analyzed at various incident angles. All data were collected with a Scintag Model 2000 XRD system (Scintag Inc., Cupertino, CA) using copper  $K\alpha$  radiation with a solid state analysis filter. The grazing incidence attachment consisted of an exit slit with  $0.3^\circ$  divergence. The step size was  $0.1^\circ$  with step times of 3, 9, or 18 s per step. The x-ray angles of incidence were set at  $0.75^\circ$  (18 s/step),  $1.5^\circ$  (18 s/step),  $5^\circ$  (9 s/step), and  $20^\circ$  (3 s/step). Because the source is fixed, the geometry of the system constrains the measurable  $2\theta$  range to 20 to  $50^\circ$ .

## 3. Results

Peak areas were obtained as a function of incident angle (Table 1). No silicon oxide was detected. This was attributed to its amorphous structure. There was no significant difference in the gold-to-platinum ratio detected at  $20^\circ$  and  $5^\circ$  angles, but a strong surface effect was detected in the  $1.5^\circ$  and  $0.75^\circ$  angles. If silicon oxide had been detectable, there may have been differences between the  $20^\circ$  and  $5^\circ$  measurements.

The relationship in Eq 3 was used to determine the expected analysis depth for gold. The mass absorption coefficient of gold was  $4018/\text{cm}$ . The  $1/e$  depth for gold as a function of incident angle is determined from Fig. 2 and summarized in Table 2. The theoretical calculations agree relatively well with the experimental data for  $0.75^\circ$ ,  $1.5^\circ$ , and  $5^\circ$  incident angles in Table 1. The lack of silicon oxide signal complicates the interpretation for  $20^\circ$ .

## 4. Discussion

Although each technique has many strong points, each also has shortcomings that need to be considered. Both principal methods heavily rely on comparison of data to published standards. XPS standards are published in various sources (Ref 15-17). The most common XRD standards are those published by International Center for Diffraction Data, ICDD (Ref 25). Frequently, standards are not available for the complex species present in multicomponent oxides. In XRD, species which are microcrystalline or amorphous will not be detected. Additionally, the top surface of an oxide, which may be responsible for significant amounts of its ultimate mechanical behavior, will

**Table 1** Area of gold and platinum diffraction peaks as a function of incident angles

	2 $\theta$ Value		Incident angle/peak area			
	Literature	Measured	20°	5°	1.5°	0.75°
Gold	38.18	38.28	427,596	5051	2245	1119
Platinum	39.76	39.79	515,758	5846	434	0
% Gold detected			45	46	84	100

**Table 2** Calculated analysis depth as a function of incident angle for gold

Incident angle	1/e depth
$0.75^\circ$	40 nm
$1.5^\circ$	70 nm
$5^\circ$	180 nm
$20^\circ$	400 nm

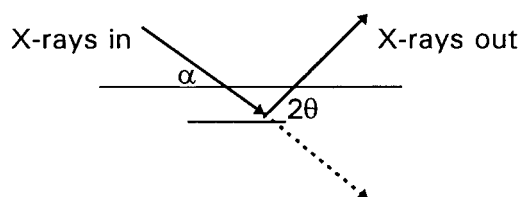


**Fig. 1** Relationship between the angle of incidence,  $\alpha$ , and twice the angle of reflection,  $2\theta$

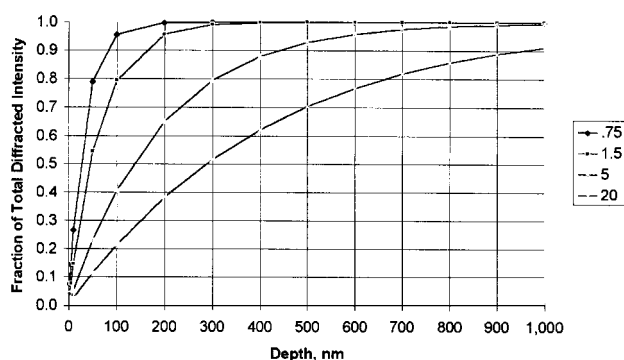


**Fig. 2** Calculated analysis depth as a function of incidence angles ( $0.75^\circ$ ,  $1.5^\circ$ ,  $5^\circ$ , and  $20^\circ$ ) for gold

not be detected with XRD, even under the most glancing conditions. Although XPS can detect composition as a function of depth, the depth profile technique can alter the species present. Deconvolution of multicomponent high energy resolution XPS peaks is operator-biased, and the presence of simple oxides can mask the presence of spinel-type structures, for example. On the other hand, the simultaneous implementation of these two techniques may be a valuable combination of procedures that can avoid many of these pitfalls while providing substantial amounts of depth-oriented information about the composition of complex oxides (Ref 13).

Quantitative statements in ARXRD must be made with considerable caution. This is especially true if there is any preferred orientation or amorphous structures in the material. For example, if a material was composed of hexagonal crystals with the c-axis aligned perfectly at the 90° to the sample surface, the extreme glancing angle of the x-ray could be essentially parallel to the basal plane, eliminating any diffraction from that plane.

Relative to many analysis techniques, the spot size of both ARXRD and XPS is somewhat large. Although XRD-microdiffraction systems currently exist with an analysis area of 30 μm, spot sizes of 1 cm are still routine in most systems available today. The use of the angle-resolved mode increases the spot size somewhat. Many XPS systems also have a large analysis diameter; once again, on the order of 0.5 cm is relatively common. Smaller spot sizes are available on many XPS systems through the use of slits, but the signal-to-noise is reduced and the analysis time dramatically increased. Current state-of-the-art XPS systems use x-ray beams focused and scanned through the use of curved lenses, with a resultant 10 μm spot size (Ref 26). To reiterate, regardless of the spot size of these techniques, XPS has a depth of analysis of 3 to 5 nm and standard XRD has a depth of analysis of a few micrometers.

It is important to keep in mind that, rather than discrete depths, the ARXRD 1/e depths are volume depths and include information from the surface to that depth, and even somewhat beyond. As discussed earlier, surface roughness of these samples complicates the depth measurements obtained from XPS. However, despite their shortcoming, the two techniques, under proper experimental conditions, can yield dovetailed information about the surface and near-surface composition of the oxide layer.

## 5. Conclusions

Although it is possible to interpret data based upon anticipated reactions, the combined use of XPS and XRD can be extremely beneficial in the identification of near-surface species. The terminology of angle-resolved x-ray diffraction, rather than the conventional grazing-angle x-ray diffraction (GXRD), has been adopted because incident angles may be much greater than that typically called grazing. The present terminology was chosen because of its correspondence to the familiar use of angle-resolved XPS for the depth profiling of thin surface layers (Ref 13).

It has been demonstrated (Ref 13) that the combined use of XPS and ARXRD is an effective method for studying complex oxide layers on multicomponent Pd-Ga based dental alloys.

The techniques were mutually beneficial in identifying features that did not correlate to published standards. The experiments helped to hypothesize the mechanism of oxide layer growth. XPS, combined with depth profiling, provides information from the surface to subsurface, while ARXRD profiles from the subsurface to the bulk.

## Acknowledgment

Support for this investigation was received from research grant DE10147 from the National Institute of Dental Research, Bethesda, Maryland.

## References

1. L.D. Madsen and L. Weaver, Examination of Titanium Oxides, Lead Oxides, and Lead Titanates using X-Ray Diffraction and Raman Spectroscopy, *Mater. Res. Soc. Symp. Proc.*, Vol 310, 1993, p 385-390
2. A.Z. Moshfegh and A. Ignatiev, Formation and Characterization of Thin-Film Vanadium Oxides: Auger Electron Spectroscopy, X-Ray Photoelectron Spectroscopy, X-Ray Diffraction, Scanning Electron Microscopy, and Optical Reflectance Studies, *Thin Solid Films*, Vol 198 (No. 1 and 2), 1991, p 251-268
3. C. Onneby and C.G. Pantano, Silicon Oxycarbide Formation on SiC Surfaces and at the SiC/SiO<sub>2</sub> Interface, *J. Vac. Sci. Technol., A*, Vol 15 (No. 3), 1997, p 1597-1602
4. S.W. Gaarenstroom, Growth and Characterization of Aluminum Oxide Thin Films for Evaluation as Reference Materials, *J. Vac. Sci. Technol., A*, Vol 15, 1997, p 470-477
5. M.N. Islam, T.B. Ghosh, K.L. Chopra, and H.N. Acharya, XPS and X-Ray Diffraction Studies of Aluminum-Doped Zinc Oxide Transparent Conducting Films, *Thin Solid Films*, Vol 280, 1996, p 20-25
6. K. Asami and K. Hashimoto, The X-Ray Photoelectron Spectra of Several Oxides of Iron and Chromium, *Corros. Sci.*, Vol 17, 1977, p 559-570
7. R.P. Goehner and M.O. Eatough, A Study of Grazing Incidence Configurations and Their Effect on X-Ray Diffraction Data, *Powder Diffr.*, Vol 7, 1992, p 2-5
8. M. Brunel and F. DeBergevin, X-Ray Beam Diffraction at Grazing Incidence, *Acta Crystallogr.*, Vol A42, 1986, p 299-303 (in French)
9. D.G. Neerincx and T.J. Vink, Depth Profiling of Thin ITO Films by Grazing Incidence X-Ray Diffraction, *Thin Solid Films*, Vol 278, 1996, p 12-17
10. M.F. Toney and T.C. Huang, X-Ray Depth Profiling of Iron Oxide Thin Films, *J. Mater. Res.*, Vol 3, 1988, p 351-356
11. R.P. Goehner, M.O. Eatough, B.A. Tuttle, and T.J. Headley, *Adv. in X-Ray Analysis*, Vol 35, 1992, p 159-167
12. F. Pons, S. Megtert, J.C. Pivin, M. Pequignot, D. Mairey, and C. Roques-Carmes, Application of a Grazing-Incidence X-Ray Diffraction Technique to the Depth-Resolved Analysis of Structural Transformations due to Surface Treatment, *J. Appl. Crystallogr.*, Vol 21, 1988, p 197-205
13. S.J. Kerber, T.L. Barr, G.P. Mann, W.A. Brantley, E. Papazoglou, and J.C. Mitchell, The Complementary Nature of X-Ray Photoelectron Spectroscopy and Angle-Resolved X-Ray Diffraction—Part II: Analysis of Oxides on Dental Alloys, *J. Mater. Eng. Perform.*, Vol 7 (No. 3), 1998, p 334-342
14. C.S. Fadley, Angle-Resolved X-Ray Photoelectron Spectroscopy, *Prog. Surf. Sci.*, Vol 16, 1984, p 275-388
15. C.D. Wagner, in *Practical Surface Analysis by Auger and X-Ray Photoelectron Spectroscopy*, D. Briggs and M.P. Seah, Ed., John Wiley & Sons, 1983, p 477-509

16. J.F. Moulder, W.F. Stickle, P.E. Sobol, and K.D. Bomben, *Handbook of X-Ray Photoelectron Spectroscopy*, Physical Electronics, Inc., 1995
17. T.L. Barr, *Modern ESCA*, CRC Press, 1994, p 339
18. S.J. Kerber, J.J. Bruckner, K. Wozniak, S. Seal, and T.L. Barr, The Nature of Hydrogen in XPS: General Patterns from Hydroxides to Hydrogen Bonding, *J. Vac. Sci. Technol. A.*, Vol 14, 1996, p 1314-1320
19. C.D. Wagner, in *Practical Surface Analysis by Auger and X-Ray Photoelectron Spectroscopy*, D. Briggs and M.P. Seah, Ed., John Wiley & Sons, 1983, p 511-514
20. T.J. Chuang, C.R. Brundle, and K. Wandelt, An X-Ray Photoelectron Spectroscopy Study of the Chemical Changes in Oxide and Hydroxide Surfaces Induced by Ar<sup>+</sup> Ion Bombardment, *Thin Solid Films*, Vol 53, 1978, p 19-27
21. K.S. Kim, W.E. Baitinger, J.W. Amy, and N. Winograd, ESCA Studies of Metal-Oxygen Surfaces using Argon and Oxygen Ion-Bombardment, *J. Electron Spectrosc. Relat. Phenom.*, Vol 4, 1974, p 351-367
22. S. Mroczkowski (Kerber) and D. Lichtman, Quantitative AES of Binary Alloys, A Comparison Between Handbook and Pseudo-First Principles Corrections, *Surface Sci.*, Vol 127, 1983, p 159-166
23. L.V. Azároff, *Elements of X-Ray Crystallography*, McGraw-Hill Book Co., 1968, p 549
24. B.D. Cullity, *Elements of X-Ray Diffraction, 2nd ed.*, Addison-Wesley, 1978, p 188
25. International Center for Diffraction Data, formerly Joint Committee on Powder Diffraction Standards, Swarthmore, PA
26. Physical Electronics Quantum 2000 ESCA Microprobe